Al-Nahrain Journal of Science
ANJS, Vol. 28(2), June, 2025, pp. 144-149

Preparation and Characterization of CuO Nanoparticles Prepared Using Plasma Jet Method

Shaimaa Fadhil Mohammed*, Rudainah Ali Lateef, Olfat Ahmad Mahmood

Department of Physics, College of Science, University of Diyala, Diyala, Iraq

Article's Information

Received: 09.09.2024
Accepted: 23.02.2025
Published: 15.06.2025

Keywords:
Optical properties
Structural properties
Band gap
CuO NPs
Plasma jets
nanostructure

Abstract

In this study, copper oxide nanostructures were created using argon plasma jets. Many methods include X-ray diffraction (XRD), Fourier transform infrared (FTIR), and ultraviolet and visible spectroscopy. The XRD pattern of the prepared CuO NPs, and the peaks obtained from CuO nanoparticles were detected at (2θ = 32.69°, 35.73°, 38.92°, 46.49°, 49.06°, 51.62°, and 53.71°) 58.66°, 61.86°, 66.12°, 66.74°, 68.50°, 72.93°, and 75.40° for levels (110) (111⁻) (111) (112⁻) (202⁻) (112) (020) (202) (113⁻) (022) (311⁻) (220) (311) (004). These obtained peaks correspond to the crystal structure monoclinic type with lattice constants (a = 4.6350, b = 3.4100, and c = 5.1080 A°), space group (C 12/C 1 no. 15), and crystalline angles (α= γ= 90°, β= 99.48°) that closely matched the standard data (JCPDS 96-101-1149). The obtained XRD results of prepared CuO nanoparticles confirmed that the typical crystalline size of CuO nanoparticles is about (24.36 nm). FTIR spectrum showed the main vibration characteristic peaks at 424, 574, 1635, 2352 and 3268cm^{-1} of the synthesized CuO NPs. The obtained broad bands referred to the structures of copper oxides consisting of nanocrystals. The detected CuO nanostructures' UV-Vis findings showed a wide peak of absorption within the wavelength extending from 300 cm^{-1} to 400 cm^{-1}, and calculated band gap energy equal to (1.4 eV).

http://doi.org/10.22401/ANJS.28.2.14
*Corresponding author: shfm1601@gmail.com

1. Introduction

The photovoltaic, electrical, magnetic, thermal, electrochemical, photocatalytic and catalytic properties of oxides have led to significant progress in the use of non-thermal plasmas in many fields and applications, including photovoltaics (solar cells and diagnostic sensors), conductive applications (conductive inks), and cosmetics. Among the nanoparticles, copper oxide nanoparticles (CuO NPs) have received much attention in this regard [1]. Atmospheric pressure non-thermal plasma jets (APPJs) have low gas temperatures and are therefore called cold plasmas. Reactive species are present in the plasma plume generated by the inert gas flow that creates a glow in the surrounding air. Due to their beneficial properties, they have shown great potential in industrial fields, such as those involving tissue processing, low-temperature sensitive cells, polymers and electronics [2–3].The non-thermal plasma is an ecologically benign alternative to the chemical synthesis of metal nanostructure materials [4, 5]. Compared with other methods of creating nanoparticles, plasma provides several benefits, including reduced operating and maintenance costs, shorter processing time, and the absence of waste or hazardous substances [6]. Considering that the characteristics of metal oxide nanoparticles are frequently different from those of bulk materials, scientists and users are interested in them [7]. This work aims to study part of copper oxides' optical and structural characteristics nanostructures and explain the mechanism by which these nanostructures are created via plasma interaction with copper in the presence of water.

2. Materials and Method

A plasma jet was used to create CuO NPs. (Figure 1) the plasma system diagram is shown with a picture of the discharge. The device was a stainless steel tube (anode) with an internal diameter of (0.6 mm) and a tube length of (7 cm) and located three centimeters from the front of the cathode. A copper plate of width

(3 cm) and length (7 cm) was used as the positive electrode and immersed in a vacuum ($2cm^2$) with a distance of 3 mm separating the needle tip from the surface of the liquid (deionized water). The syringe attached to the argon is discharging gas. The reaction was an acquired glass vessel (5.5 cm in width and 8.5 cm in length), after which distilled water was used to clean the polished copper electrode. The copper strip was subsequently immersed in an electrolyzer, where an AC power source provided a voltage of 10 kV at a frequency of 8.4 kHz to initiate the discharge current used for discharge was 4 to 8 mA. The copper strip was immersed in distilled water for approximately 20 mL and then bombarded with plasma at different times until a slight color change in the water appeared. That is, the electrolysis system was exposed for (3 minutes). As seen in (Figure2), the electrolyte's color altered.

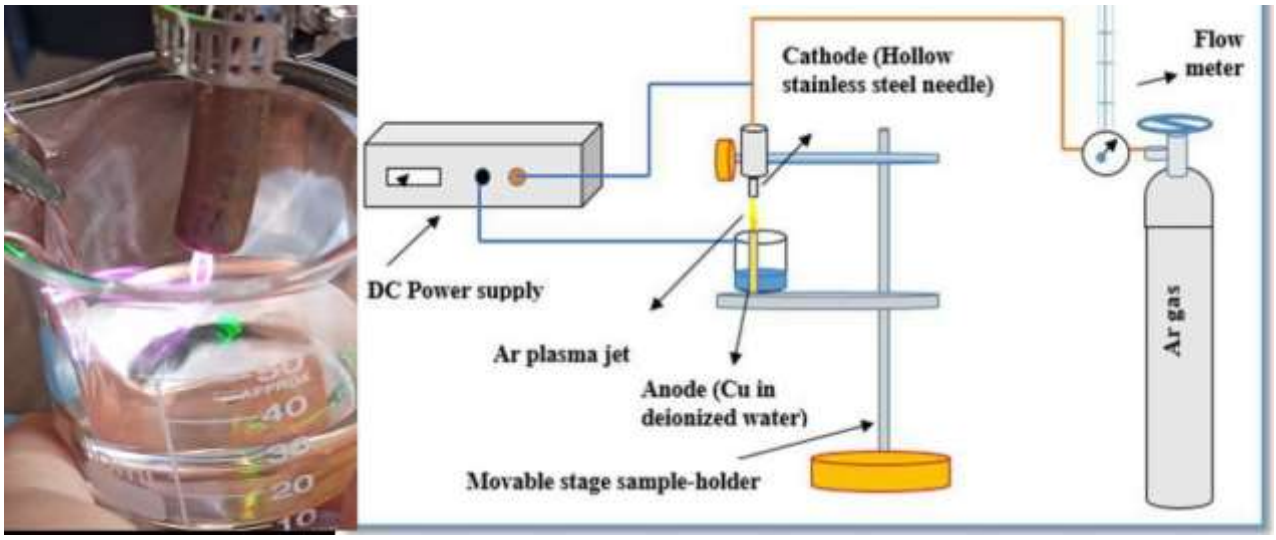

Figure 1. Schematic of plasma jet.

Figure 2. (Online color) Discharge duration (3 minutes). 5 mA is the discharge current. The distance is 3 mm.

3. Results and Discussion

The detected XRD peaks at the diffraction angle (2θ°) verified the prepared nanoparticles using the argon atmospheric plasma jet (AAPJ), to determine the crystal structure type and phase purity, and compared with the JCPDS standard card. Figure 3 presents the characteristic XRD peaks of synthesized CuO NPs.

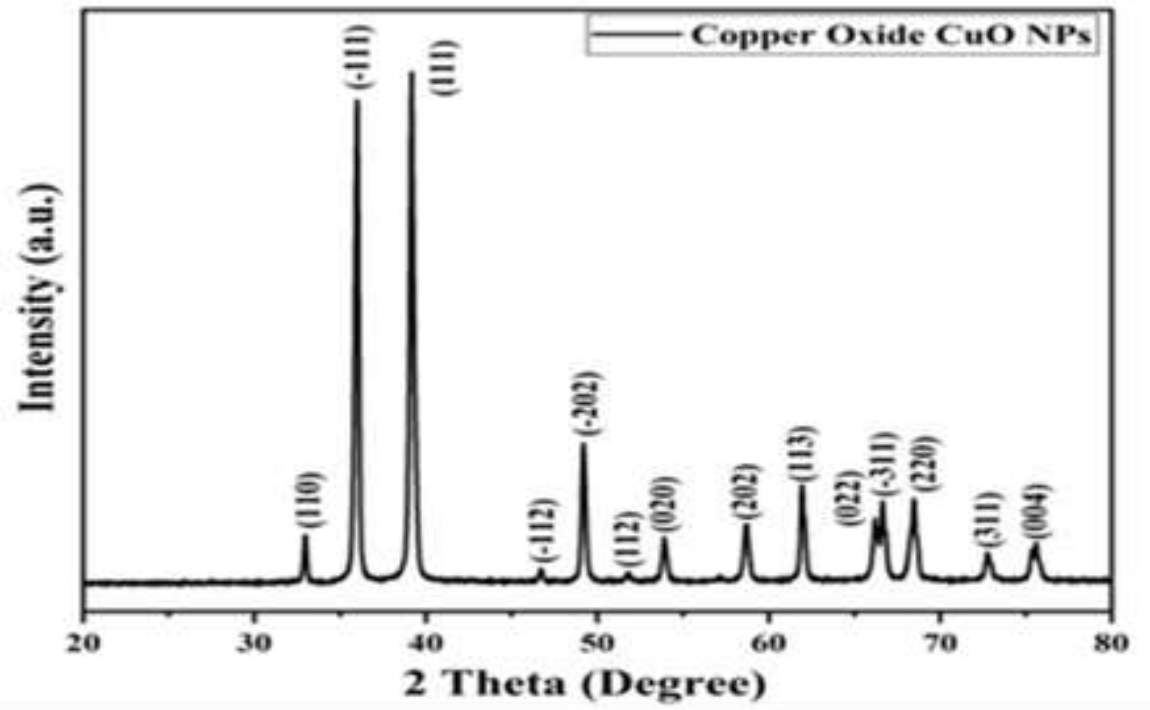

Figure 3. XRD pattern of the prepared copper oxide nanoparticles (CuO NPs)

The obtained detected at (2θ = 32.69°, 35.73°, 38.92°, 46.49°, 49.06°, 51.62°, and 53.71°) 58.66°, 61.86°, 66.12°, 66.74°, 68.50°, 72.93°, and 75.40° for levels (110) (111⁻) (111) (112⁻) (202⁻) (112) (020) (202) (113⁻) (022) (311⁻) (220) (311) (004). These characteristic peaks corresponded with the monoclinic type structure, space group (C 12/C 1 no. 15), and lattice constants (a = 4.6350 A°, b = 3.4100 A°, and c = 5.1080 A°), and crystalline angles (CuO NPs' peaks were α= γ= 90°, β= 99.48°), these detected peaks were consistent with the reference data (JCPDS 96-101-1149). The observed XRD results for the prepared CuO NPs proved that no impurity peaks were detected; indicating high-purity CuO NPs.

From the Debye-Scherrer formula, the crystalline size was estimated for the synthesized CuO NPs.

$$FWHM\ (2\theta) = \left(\frac{K\,\lambda}{L\,\cos\theta}\right) \quad \ldots(1)$$

where K is a unitless constant that depends on the shape of the crystal and is often of the order of = 0.9… L/ peak width at average height... θ/ Bragg angle.λ / Wavelength (nm). Furthermore, CuO NPs' crystalline size is about (24.36 nm). Table 1 represents the XRD calculations of the synthesized CuO NPs. The FT-IR, or Fourier transform infrared spectroscopy, was used to examine the functional groups within the prepared CuO NPs in this work. The formation of chemical bonds within the CuO NPs structure was detected.

Table 1. The XRD calculations of the synthesized CuO samples.

2Θ Standard (deg)	2 Θ Experimental (deg)	FWHM (deg)	d-space Standard	d-space Experimental	Crystalline Size (nm)	hkl
Copper Oxide Nanoparticles (CuO NPs)						
35.73	35.96	0.2749	2.5108	2.4954	27.51	(002)
38.92	39.17	0.3246	2.3117	2.2985	23.07	(111)
49.06	49.21	0.2821	1.8553	1.8553	25.61	(-202)
61.86	61.98	0.3206	1.4985	1.4986	21.25	(-113)

The FT-IR spectrum was recorded inside the 400 wavenumber range to 4000 cm^{-1} (see figure 4). The FT-IR peak was acquired, and the spectrum presented the vibrations bonds of the O-H bond, C=C bond and Cu-O bond within the CuO structure. Therefore, CuO nanoparticles were successfully fabricated using the plasma (jetting) method. The characterization of the surface functional groups of the biotinylated copper nanoparticles is presented in (figure 4). The characteristic vibration bands were detected at (424, 574, 1635, 2352 and 3268 cm^{-1}). The strongest bands at (3268 and 1635 cm^{-1} due to the vibrations of the copper-oxide bond [11]. The peak at (710 cm^{-1}) is ascribed to Cu-O bond vibrations, which proved the existence of the metal oxide group within the prepared CuO NPs. The presence of a hydroxide group in the sample was confirmed by the vibration peak at (3268 cm^{-1}). This finding can be attributed to water, it is a chemical by-product that adheres to the surface of copper nanoparticles and can be vaporized by further heating.

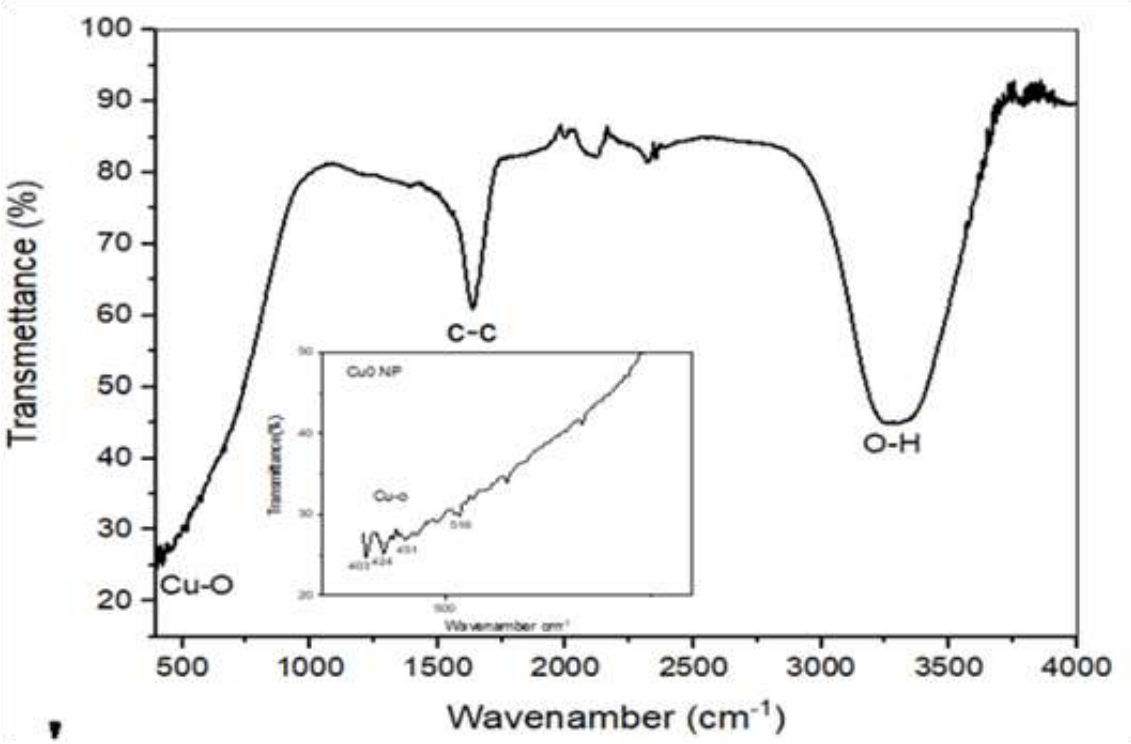

Figure 4. CuO NPs' FTIR spectra.

The UV spectroscopy was utilized to investigate the optical characteristics of synthesized CuO nanostructures by the (AAPJ) preparation approach. The optical characterisation reveals the specifics of the band gap energy and absorption of CuO nanoparticleThe band gap energy is considered one of the most important features, in addition to the absorption aspect when studying the optical characteristics. The band gap energy was estimated using Planck's formula, which can be found in equation (1) [5].

$$E_g = \frac{hc}{\lambda} = \frac{1240}{\lambda} \quad \dots (2)$$

where (h) represents the Planck's constant of (6.626×10^{-34} J.s), (Eg) is the energy band gap, (c) explains the velocity of light (3×10^{8} m/s), and (λ) represents the wavelength that can be estimated from the linear portion of the absorbance spectrum. From the obtained UV–Vis spectrum of prepared CuO NPs, A wide-ranging absorption band extending from the wavelength (300 nm) to (400 nm) (Figure 5). The optical absorption band moved to a longer wavelength (red shift) compared with the absorption band of the bulk CuO [10]. The CuO nanoparticles' absorption coefficients were visually computed using Tauc's relation, as presented in equation (2), for direct transitions [9].

$$(\alpha h\nu)^r = A(h\nu - E_g) \quad \dots (3)$$

The band gap energy is represented by (Eg), whereas (α) explains the absorption coefficient, (r) is the value of direct transition (r = 2), (ν) is photon frequency and (A) is a constant of (0.9). A common method for determining the band gap energy is illustrated in

Figure (6), where the (x) axis is used to intercept the linear extrapolation portion and consider the relationship between $(\alpha h\nu)^r$ And photon energy (hv). Energy of The spacing between the bands was estimated to be (1.4 eV), this value is lower than the band gap observed in the literature [8, 9].

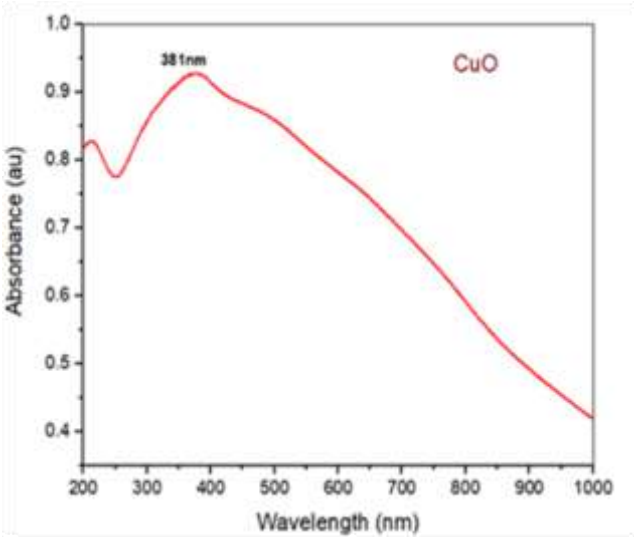

Figure 5. CuO nanoparticles' optical absorption spectrum.

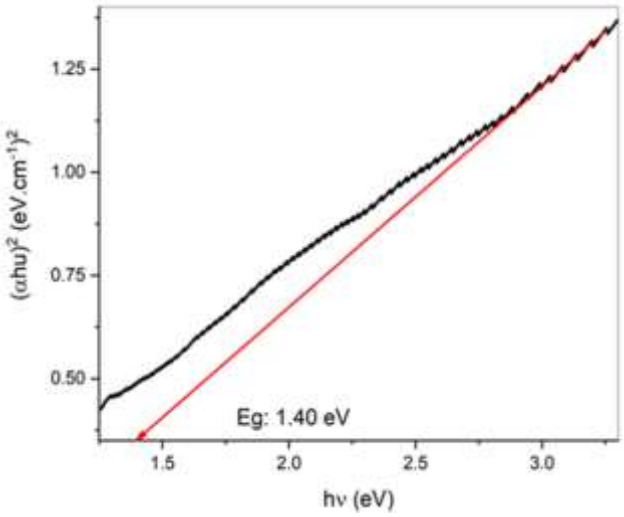

Figure 6. CuO nanoparticles' band gap energy

4. Conclusions

Argon plasma jetting has successfully produced pure and crystalline CuO NPs, with an average crystalline size is (24.36 nm). The synthesized CuO NPs in this report demonstrated that the nanoparticles recorded high activity in the visible light for photovoltaics, and showed excellent absorption and band gap energy characteristics. Based on XRD and FTIR, CuO found in nucleophilic compounds has mass transfer.

Acknowledgements: I would like to thank everyone who contributed to the completion of the research from the Chemistry Laboratory in the College of Science (University of Diyala), the BPC office in Adhamiyah in Baghdad and the Al-Khawrah office in Yarmouk in Baghdad.

Conflicts of Interest: The authors confirm that there is no conflict of interest regarding this work. .

References

[1] Hamdan, A.; Agati, M.; Boninelli, S.; "Selective Synthesis of 2D Mesoporous CuO Agglomerates by Pulsed Spark Discharge in Water". Plasma Chemistry and Plasma Processing, 41: 433–445, 2021.

[2] Liu, F.; Zhang, B.; Fang,.; Wan, M.; Wan, H.; Ostrikov, K.; "Jet-to-jet interactions in atmospheric pressure plasma jet arrays for surface processing". Plasma processes and polymers, 15(1): 1-11,2017.

[3] Lietz, M. A.; Damany, X.; Robert, E.; Pouvesle, J. M.; Kushner, M. J.; "Ionization Wave Propagation in an Atmospheric Pressure Plasma Multi-jet". Plasma Sources Science and Technology, vol. 28, pp. 1-57, 2019.

[4] Nguyen, J. L. N.; Lamichhane, P.; Choi, E. H.; Lee, G. J.; " Structural and Optical Sensing Properties of Nonthermal Atmospheric Plasma-Synthesized Polyethylene Glycol Functionalized Gold Nanoparticles". Nanomaterials 11: 1678, 2021.

[5] Mohammed, R. S.; Aadim, K. A.; Ahmed, Kh. A.; "Synthesis of CuO/ZnO and MgO/ZnO Core/Shell Nanoparticles with Plasma Jets and Study of their Structural and Optical Properties". Karbala International Journal of Modern Science, 8: 213-222, 2022.

[6] Murbat, T H. H.; Abdalameer, N. KH.; Brrd, A. Kh.; Abdulameer, F.; "Effects of Non Thermal Argon Plasma Produced at Atmospheric Pressure on the Optical Properties of CdO Thin Films". Baghdad Science Journal, 15(2): 221-226, 2018.

[7] Primc, G.; Brencic, K.; Mozeti, M.; Gorjanc, M.; "Recent advances in the Plasma-Assisted Synthesis of Zinc Oxide Nanoparticles". Nanomaterials, 11: 1191, 2021.

[8] Hasan, F. A.; Hussein, M. T.; Abdulsattar, M. A.; "Structural, Optical, and Morphological Study of the Zinc Oxide Nano-Thin Films with Different Thickness Prepared by Pulsed Laser Deposition

Technique". Iraqi Journal of Science, 63(12): 5242-5254, 2022.

[9] El-Trass, A.; Elshamy, H.; Mehasseb, I.; El-Kemary, M.; "CuO Nanoparticles: Synthesis, Characterization, Optical Properties and Interaction with Amino Acids". Appl. Surf. Sci., 258: 2997–3001, 2012.

[10] Tharchanaa, S. B.; Priyanka, K.; Preethi, K.; Shanmugavelayutham, G.; "Facile synthesis of Cu and CuO nanoparticles from copper scrap using plasma arc discharge method and evaluation of antibacterial activity". Materials Technology, 36(2): 97-104, 2021.

[11] Kumar, P. V.; Shameem, U.; Kollu, P.; Kalyani, R.L.; Pammi, S.V.N.; "Green synthesis of CuO NPs using Aloe vera leaf extract and its antibacterial activity against fish bacterial pathogens", Bio. Nano Science, 5(3): 135-139, 2015.